

miR-34a Silences c-SRC to Attenuate Tumor Growth in Triple Negative Breast Cancer

Brian D. Adams^{1,10}, Vikram B. Wali², Christopher J. Cheng^{1,3,11}, Sachi Inukai⁴, Carmen J. Booth⁵, Seema Agarwal^{6,12}, David L. Rimm⁶, Balázs Győrffy^{7,8}, Libero Santarpia⁹, Lajos Pusztai², W. Mark Saltzman³, and Frank J. Slack^{4,13}

¹Department of Molecular, Cellular and Developmental Biology, Yale University, New Haven, Connecticut 06511, USA.

²Yale Cancer Center Genetics and Genomics Program, Yale University School of Medicine, New Haven, Connecticut 06520, USA.

³Department of Biomedical Engineering, Yale University, New Haven, Connecticut 06511, USA.

⁴Institute for RNA Medicine, Beth Israel Deaconess Medical Center, Harvard Medical School, Boston, Massachusetts 02215, USA.

⁵Section of Comparative Medicine, Yale University School of Medicine, New Haven, Connecticut 06520, USA.

⁶Department of Pathology, Yale University School of Medicine, New Haven, Connecticut 06520, USA.

⁷nd Department of Pediatrics, Semmelweis University, Tűzoltó u. 7-9, H-1094, Budapest, Hungary.

⁸MTA TTK Lendület Cancer Biomarker Research Group, Magyar Tudósok körútja 2., 1117, Budapest, Hungary

⁹Humanitas Clinical and Research Institute, Via Manzoni 113A, 20089 Rozzano, Milan - Italy

Current Address:

¹⁰Department of Pathology, Beth Israel Deaconess Medical Center, Boston, Massachusetts 02115, USA

¹¹Alexion Pharmaceuticals, Inc., 352 Knotter Drive, Cheshire, Connecticut 06410, USA

¹²Department of Pathology, Georgetown University, Washington, DC 20007, USA

Running Title: miR-34a Shows Tumor Suppressor Functions in TNBC

Keywords: microRNAs, Triple Negative Breast Cancer, SRC, miR-34a, Dasatinib

Financial Support: This work was supported by a pilot grant from the Yale Cancer Center, and from NIH grants to FJS (R01 CA157749 and R01 CA131301), DR (P30 CA016359-35S2), and MS (R01 CA149128). LP was supported by (Breast Cancer Research Foundation Award), BG by the OTKA K108655 grant, and LS by AIRC Grant 6251.

¹³**Corresponding Author:** Frank Slack, Ph.D.

Department of Pathology, BIDMC Cancer Center/Harvard Medical School, 3 Blackfan Cir (CLS412), Boston, MA 02115

Telephone: 617-735-2601; **Fax:** 617-735-2646; **Email:** fslack@bidmc.harvard.edu

Disclosure of Conflicts of Interest: FJS is an advisor and shareholder in Mirna Therapeutics, which is conducting clinical trials with miR-34 in liver cancer. Other authors have no conflicts of interest to disclose.

Word Count: 5490

Total Figures: 6

Total Tables: 1

Abstract:

Triple-negative breast cancer (TNBC) is an aggressive subtype with no clinically proven biologically targeted treatment options. The molecular heterogeneity of TNBC and lack of high frequency driver mutations other than *TP53* have hindered the development of new and effective therapies that significantly improve patient outcomes. MicroRNAs (miRNAs), global regulators of survival and proliferation pathways important in tumor development and maintenance, are becoming promising therapeutic agents. We performed miRNA-profiling studies in different TNBC subtypes to identify miRNAs that significantly contribute to disease progression. We found that miR-34a was lost in TNBC, specifically within mesenchymal and mesenchymal-stem cell like subtypes, whereas expression of miR-34a targets were significantly enriched. Furthermore, restoration of miR-34a in cell lines representing these subtypes inhibited proliferation and invasion, activated senescence, and promoted sensitivity to dasatinib by targeting the proto-oncogene c-SRC. Notably, SRC-depletion in TNBC cell lines phenocopied the effects of miR-34a re-introduction, while SRC overexpression rescued the anti-tumorigenic properties mediated by miR-34a. miR-34a levels also increased when cells were treated with c-SRC inhibitors, suggesting a negative-feedback exists between miR-34a and c-SRC. Moreover, miR-34a administration significantly delayed tumor growth of subcutaneously and orthotopically implanted tumors in nude mice, and was accompanied by c-SRC downregulation. Finally, we found that miR-34a and *SRC* levels were inversely correlated in human tumor specimens. Together, our results demonstrate that miR-34a exerts potent anti-tumorigenic effects *in vitro* and *in vivo*, and suggests that miR-34a replacement therapy, which is currently being tested in human clinical trials, represents a promising therapeutic strategy for TNBC.

Introduction:

Triple-negative breast cancer (TNBC) comprises ~20% of breast cancers and accounts for a disproportionate share of morbidity because of its aggressive behavior, increased incidence in younger women, and lack of effective targeted therapies(1–4). This breast cancer subset is defined by what it lacks: estrogen-receptor, progesterone-receptor, and HER2 amplification, thereby limiting systemic treatment options for these patients to conventional chemotherapy. Transcriptional profiling studies initially suggested TNBC represented a distinct molecular entity that was different from ER-positive luminal-A type cancers(5). It has recently become apparent TNBC itself is a molecularly heterogeneous disease and is often subdivided into smaller categories including mesenchymal/mesenchymal stem cell-like (M/MSL), luminal androgen receptor type (LAR), and basal-like (BL) with or without an extensive immunomodulatory (IM) component(6–8). Despite identifying the molecular pathways dysregulated in TNBC, this extensive transcriptional and genomic heterogeneity has limited the development of broad therapeutic strategies for treating patients with TNBC. Therefore, discovery of a single therapeutic molecule that can function to suppress the multiple pathways supporting TNBC growth would be an important clinical breakthrough.

Since miRNAs target multiple pathways and function as signal modulators by fine-tuning gene expression to mediate tumor-suppressive phenotypes, these molecules represent attractive therapeutic options and targets. MiRNAs represent a class of small non-coding RNAs that function as global regulators of gene expression and are important master controllers of cell survival and proliferation pathways critically important in cancer development and tumor maintenance(9). These ~22 nucleotide, non-coding RNAs control the expression of protein coding genes via imperfect binding to the 3' untranslated region (3'UTR) of the target messenger RNA (mRNA), leading to either translational inhibition or degradation(10). Some studies estimate miRNAs regulate $\geq 60\%$ of the human protein-coding transcriptome(11). Importantly, single miRNAs can regulate entire cell signaling networks in a cell-context dependent manner(12). Since miRNAs can function as oncogenes or tumor suppressors, and can control the robustness of multiple cell signaling

pathways(13,14), miRNAs that become dysregulated could promote a disease state, such as cancer. Our goal was to identify the key miRNAs dysregulated in TNBC in an effort to elucidate the disease and potentially point to novel miRNA-based therapeutics. We found miR-34a was selectively lost in TNBC cells and harbored tumor-suppressive functions when re-introduced into TNBC cells, with the most robust cell killing occurring in the mesenchymal-TNBC subtypes.

While there have been historical challenges associated with the use of RNA in therapy, chemical modifications to the backbone of synthetic RNA molecules in combination with advances in nanoparticle-based delivery methodologies, have resulted in significantly increased half-lives *in vivo* and better therapeutic potential. Lipid- and polymer-based nanoparticle systems can now be used to effectively deliver RNA molecules into tumor cells(15–18). Here we used a polyamine-co-ester terpolymer nanoparticle (tNP) technology, previously shown to actively target plasmid DNA to tumor cells(19), as a safe and effective method for delivering synthetic miR-34a into TNBC tumor cells *in vivo*. From the combination of our *in vitro* and *in vivo* studies, we found miR-34a ameliorates multiple tumor phenotypes, and acts through the regulation of mRNA targets such as *BCL2*, *NOTCH1*, and a novel target *SRC*. Moreover, this miR-34a effect occurs specifically in the mesenchymal-TNBC subtype, and can sensitize these cells to therapeutic agents such as dasatinib and paclitaxel.

Materials and Methods:

Cell Culture

All breast cancer cell lines were purchased directly from ATCC in 2013 and maintained in DMEM supplemented with 10% FBS, 1% Pen/Strep and cultured at 37°C in a 5% CO₂ incubator. All experiments were performed within 6 months to 1 year upon receipt of cells, and characterization by STR analysis was performed by ATCC. Normal breast conditionally reprogrammed cell lines (CRCs) were maintained without co-culturing with feeder cells(20). HMECs (Life Technologies) were maintained as per manufacture's protocol, while MCF-10A cells were cultured in a defined media(21). For RNA-based functional experiments, *mirVana* mimics and validated Silencer Select

siRNAs (Life Technologies) were transfected into 5×10^4 cells using DharmaFECT 1 (GE Healthcare Dharmacon), as per manufacture's protocol. For extended experimental procedures see

Supplementary Materials and Methods.

Quantitative Real Time PCR

For qPCR, cells were lysed in TRIzol (Life Technologies), and total RNA was used as the input for subsequent RT-PCR reactions. For miRNA analysis, cDNA synthesis and qRT-PCR were performed according to the miScript II RT Kit (Qiagen) and miScript SYBR® Green PCR Kit (Qiagen) protocols respectively. For mRNA analysis, cDNA synthesis and qRT-PCR were performed according to the RT² First Strand Kit and RT² qPCR Primer assay protocols (Qiagen).

Cell Viability

For assessment of cytotoxicity and development of IC₅₀ curves, Sulforhodamine Blue (SRB) assays were performed as previously described(22), see *Extended Experimental Procedures*. For morphological assessments, cells were stained with 0.2% crystal violet for 10 min at room temperature, and washed with PBS. Images were acquired using a Zeiss dissection microscope (Zeiss, Jena, Germany), AxioCam MRc 5 camera (Zeiss) and AxioVision 4.7.1 imaging software (Zeiss). In some instances, stained cells were treated with 10% acetic acid with 0.1% SDS and dye abundance was quantified by measuring absorbance at 600nm.

Invasion and Soft Agar Assays

For invasion assays, following miRNA or siRNA transfection, cells were cultured in 0.1% serum containing media overnight, and then seeded into BD BioCoat™ BD Matrigel™ Invasion Chambers. For soft agar assays, following miRNA or siRNA transfection, cells were mixed with agarose to a 0.3% concentration in RPMI growth media, and cultured for 25 days. At the end of the study, inserts or cells were fixed, stained with crystal violet, and counted.

SA- β -Gal Assays

Following miRNA or siRNA transfection, cells were seeded into 12-well plates. After 5-6 days, cells were assessed for cellular β -galactosidase activity, using a Senescence β -Galactosidase Staining Kit (Cell Signaling Technology). Five randomly designated areas in each well were then scored for the proportion of cells containing a blue precipitate (cleaved X-gal) as compared to the total number of cells within the same field.

Animal Maintenance and Treatment

5- to 6-week-old female *CrTac:NCr-Foxn1^{nu}* mice (Taconic) were maintained at Yale University in accordance with Yale Animal Resource Center and Institutional Animal Care and Use Committee guidelines. For tumor formation, miRNA treatments, and tumor analysis see *Extended Experimental Procedures*.

Luciferase Targeting Assays

For miRNA targeting assays, HEK-293T cells were transfected with a pLightSwitch-SRC-3'UTR plasmid or an pLightSwitch-Empty-3'UTR control (SwitchGear Genomics), in combination with miR-34a or miR-Scr control using DharmaFECT Duo (GE Health Dharmacon). After 24 hours cells were lysed and luciferase activity measured as per manufacture's protocol. Luciferase signal was normalized to the 0nM miRNA control condition for each UTR construct. Technical quadruplicates were performed and experiments were performed three times.

Statistical Analysis

Unless otherwise stated, a student's t test was used for p value calculations. Values reported are expressed as the mean \pm SD, whereas densitometric readings of Western blot analyses are reported as averages. When more than one condition was being compared, such as changes between various treatments and control groups an ANOVA analysis was performed. Statistical significance was set at $p < 0.05$.

Results:

miR-34a is aberrantly lost and has prognostic value in TNBC

To identify miRNAs with potential therapeutic value in TNBC, we performed miRNA microarray analysis on >1000 miRNAs from 19 breast cancer cell lines. Clustering analysis of the top 50 most variant miRNAs indicated the presence of a subset of miRNAs differentially expressed between basal- and luminal-A type cell lines(**Fig. S1A**). qRT-PCR validation experiments were performed on a panel of 13 breast cancer and 9 normal breast cell lines to determine which miRNAs were differentially expressed as compared to normal cells. This included a set of conditionally reprogrammed cell (CRC) lines established from normal mammary tissue(20). A number of highly expressed TNBC-specific miRNAs were identified, such as miR-221 and miR-155, when compared to luminal-A type cells, however these miRNAs were also highly expressed in CRC lines(**Fig. S1B**). Furthermore, non-tumorigenic MCF-10A and HMEC control lines also harbored high levels of these miRNAs.

Instead, we focused on identifying miRNAs lost in TNBC with the aim of pointing us towards a possible miRNA re-introduction-based therapeutic agent. We identified miR-34a and miR-200 to be aberrantly downregulated in TNBC cell lines as compared to both luminal-A type and normal breast cell lines(**Figs. 1A & S1C**). These findings support our previous work, where we identified miR-34a to be downregulated in TNBC breast cancer patient samples(23). Furthermore, miR-200 is a known regulator of metastatic processes, and is downregulated in TNBC(24,25). Given miR-34a is specifically lost in TNBC cell lines as well as in patient samples, and that the therapeutic targets of miR-34a specific to TNBC have not yet been well defined, we selected miR-34a for further investigation.

To determine if miR-34a harbored prognostic value in TNBC patients, Kaplan-Meier survival plots and Cox regressions were computed from TCGA. High expression of miR-34a in TNBC-patients conferred better overall survival (OS) (n=97, HR=0.22, p=0.041) than in those with low miR-34a, an

effect not seen in the all-breast cancer patient cohort(**Fig. 1B-C**). Given the heterogeneity of TNBC, we investigated whether predicted targets of miR-34a were enriched in specific TNBC subtypes. We returned to the original breast cancer cell line dataset where U133A data was available for 22,283 genes across 19 cell lines. We identified a TNBC-overexpressed gene-set (264 genes) which demonstrated enrichment for miR-34 target genes(**Fig. S1D**). In addition, target enrichment of another TNBC-related miRNA, miR-200, was also identified. These miRNA targets were not enriched in the TNBC-under-expressed gene-set (*data not shown*).

We then performed hypergeometric analyses of all putative miR-34a targets across the TNBC subtype-specific gene expression (GE) profiles reported in Lehmann *et al.*(6). 3,000 predicted miR-34a targets, irrespective of site conservation, were acquired from TargetScan(26), and compared to the top 20% upregulated genes within all TNBC (~2,872 genes), and within each TNBC subtype (variable sample size). When the number of miR-34a-TNBC subtype-specific targets were compared to the total number of miR-34a-TNBC targets, hypergeometric analysis indicated an overrepresentation of miR-34a targets present in the MSL-and M-TNBC subtypes, while miR-34a targets in the LAR and immunomodulatory (IM) TNBC subtypes were substantially underrepresented(**Fig. 1D**). A stringent enrichment analysis on 760 high confidence miR-34a targets was also performed, which still resulted in significant overrepresentation occurring within the MSL-TNBC subtype(**Fig. S1E**). These data support the notion that the genes important for growth and survival within mesenchymal-TNBC cell types are highly regulated by miR-34a, and that these cells suppress miR-34a to maintain a tumorigenic state.

miR-34a is a bona-fide TNBC tumor suppressor

To determine if miR-34a promoted tumor-suppressive phenotypes in TNBC, we transfected a panel of breast cancer cell lines with 30nM miR-34a or scrambled control (miR-Scr), and assayed cell growth using SRB assays(22). BT-549 and MDA-MB-231 TNBC growth was inhibited by miR-34a re-introduction(**Fig. 1E**), while luminal-A MCF-7, and LAR-TNBC MDA-MB-453 cells were marginally impacted. This TNBC-specific growth inhibition by miR-34a was observed in an extended

panel of TNBC lines, while normal CRCs and human fibroblasts (HFF) were not severely impacted(**Fig. S1F**). Lower IC₅₀ values were also obtained in TNBC lines versus luminal-A or LAR-TNBC cell lines(**Table 1**).

We next investigated additional anti-tumorigenic phenotypes associated with miR-34a re-introduction. The earliest phenotypic consequence, observed 36 hours after miR-34a transfection, was abrogation of invasion. Using Matrigel-coated Boyden-chamber assays, BT-549, MDA-MB-231, and MDA-MB-436 cells transfected with 5nM miR-34a resulted in ~2.1-, 4.0-, and 2.9-fold reductions in the number of invasive cells(**Figs. 2A & S2A**). This phenotype is present prior to any anti-growth effects mediated by miR-34a, which occurs >84 hours post-transfection(**Fig. 1E**), and is not a result of apoptosis(**Fig. 2C**). These data suggest miR-34a regulates cellular targets in TNBC cells important in focal adhesion and invasion, which are the same signaling pathways that define MSL- and M-TNBC subtypes.

We next tested whether miR-34a transfected TNBC cells could grow in an anchorage-independent fashion. Specifically, BT-549, MDA-MB-436, and MDA-MB-231 cells transfected with 7.5nM miR-34a resulted in ~8.2-, 4.1-, and 3.6- fold reductions in colony formation, respectively, after 20 days of culture in 0.3% soft agar(**Figs. 2B & S2B**). To determine if this phenotype was due to a block at a particular stage in cell cycle progression, we performed propidium-iodine (PI) staining assays, which indicated miR-34a transfected MDA-MB-231 cells resulted in a 5% increase of cells in G2/M 4-6 days post-transfection(**Fig. 2D**). Similar results were obtained with BrdU assays(**Fig. S2C**). Despite this marginal G2/M arrest, miR-34a transfected TNBC cells underwent striking morphological changes indicative of senescence: specifically an elongated and flattened cytoplasm(27)(*data not shown*). Senescent cells can be the result of both G1 and/or G2 arrest(27), which may explain the lack of a stage-specific block in cell cycle upon miR-34a transfection. Indeed, SA-β-gal assays performed on miR-34a transfected TNBC cells confirmed this senescence-promoting effect in a dose-dependent manner(**Figs. 2E & S2D-E**). Conversely, MCF-7 cells, which

harbor high endogenous miR-34a levels and higher baseline rates of senescence, had an ~2-fold reduction in SA- β -gal activity when treated with a miR-34a sponge(**Fig. S2F**).

To determine whether miR-34a-induced anti-tumorigenicity was due to differential transfection efficiencies, we performed psiCheck2 luciferase reporter assays, where a miR-34a sensor sequence was inserted downstream of *Renilla* luciferase. Co-transfection experiments using wild-type or mutant sensors and miR-34a or miR-Scr mimics indicated 500pM miR-34a was sufficient to reduce reporter activity by 5-10-fold across all lines tested(**Fig S2G**). Therefore, the anti-tumorigenic phenotype induced by 5-30nM of miR-34a in MSL- and M-TNBC cells likely reflects a heightened sensitivity to miR-34a re-introduction and not differential transfection efficiency. Overall these data suggest miR-34a re-introduction in TNBC shuts down oncogenic signaling pathways that affect invasion and proliferation, eventually resulting in cell death by way of cytostasis/senescence. Interestingly, some oncogenic mediators could include non-coding RNAs such as the miR-17/92 cluster, which is known to be elevated in TNBC(28–30) and can be downregulated by miR-34a re-introduction(**Fig. S2H**).

Systemic delivery of miR-34a has tumor-suppressor activity in vivo

Given the *in vitro* findings, we tested whether miR-34a could reduce tumor growth *in vivo*. MDA-MB-231 cells were mixed with Matrigel and injected into the flanks of *CrTac:NCr-Foxn1^{nu}* mice. Once tumors reached 150mm³, mice were randomized into a miR-34a or miR-Scr treatment cohort. MiRNA mimics were packaged into a neutral-lipid emulsion and injected intratumorally at a 25 μ g/tumor dose. After 3 treatments, given every four days, miR-34a tumors did not proliferate beyond pre-treatment tumor size, while miR-Scr tumors grew unperturbed(**Fig. 3A; left panel**). At the end of the study, tumors treated with miR-34a harbored an ~4.4-fold reduction in tumor weight, as compared to miR-Scr controls(**Fig. 3A; right panel**).

To test if systemic delivery of miR-34a could impact the progression of TNBC, MDA-MB-231 tumors, originally inoculated at the orthotopic mammary site were treated systemically with tNP-packaged miR-34a or miR-Scr control. After 3 treatments of a 1.5mg/kg dose every 4 days, mice

given miR-34a had significantly reduced tumor growth(**Fig. 3B**). Tumors were harvested for further analysis, and while tumor weights were only slightly decreased in the miR-34a arm, a marked reduction in Ki67 staining was observed when compared to controls(**Fig. 3E**). MiR-34a levels were elevated ~2.5-fold in the miR-34a treated tumors(**Fig. 3C**), while *bona-fide* miR-34a targets such as *JAG1* were downregulated(**Fig. 3D**). Taken together, these data indicate tNP can deliver functionally active miR-34a to tumors located at the mammary orthotopic site, resulting in miRNA-mediated phenotypes *in vivo*. To assess toxicity associated with systemic delivery of miR-34a, we collected serum from mice given miR-Scr and miR-34a treatments. Liver function tests showed no evidence of hepatic damage(**Fig. 3F**). Liver tissue architecture was also normal, and we did not find any evidence for TUNEL⁺ cells(**Fig. 3G**).

miR-34a can sensitize mesenchymal-TNBC cells to dasatinib

We next tested whether miR-34a could sensitize TNBC cells to certain front-line agents for TNBC patients. Using clonogenic assays, we found 10nM miR-34a induced variable sensitivities to 0.15-4nM paclitaxel in MDA-MB-231, BT-549, MDA-MB-453, and Hs578T cells(**Figs. 4A-C & S3B**). Although significant, this was a mild sensitization effect. Instead, given miR-34a has strong anti-tumorigenic effects in the MSL- and M-TNBC subtypes, and that these subtypes are sensitive to agents such as dasatinib due to heightened expression of focal adhesion genes such as c-SRC(6)(**Fig. S3A**), we tested whether miR-34a could synergize with dasatinib in TNBC cells. Indeed, 10nM miR-34a sensitized MDA-MB-231, BT-549, Hs578T, and MDA-MB-436 cells to 11-900nM dasatinib, as compared to miR-Scr control(**Figs. 4A-B & S3B-C**). We did not observe this sensitivity in the LAR-TNBC MDA-MB-453 cells or in HeLa cells(**Figs. 4C & S3C**), giving credence to the notion that miR-34a synergizes with dasatinib by regulating similar pathways important to the biology of mesenchymal-TNBC cells.

Given this miR-34a-dasatinib synergy, we wondered whether dasatinib could affect endogenous miR-34a levels in TNBC. MDA-MB-231 cells treated with dasatinib for 60 hours demonstrated a dose-dependent increase in miR-34a levels, with the highest fold-change being 4.4-fold in 100nM

treated cells as compared to the 0nM control(**Fig. 4D**). This effect appeared selective given miR-15a levels did not change more than 1.7-fold across any treatment condition. Dasatinib-induced miR-34a was functional as it resulted in reduced miR-34a sensor reporter activity(**Fig. 4E**), and levels of miR-34a targets such as *JAG1*(31)(**Fig. S3D**). These effects are dasatinib-specific, as paclitaxel treated MDA-MB-231 cells showed no significant increase in miR-34a levels, even at cytotoxic levels $\geq 1\text{nM}$ (**Fig. S3E**). While the mechanism(s) by which dasatinib-mediated induction of miR-34a levels occur(s) is unclear, given dasatinib is a c-SRC inhibitor, c-SRC signaling could regulate activity of a transcription factor or an RNA binding protein that controls expression, stability and turnover of miR-34a. Since we observed no active luciferase expression generated from reporters containing previously described miR-34a promoters(32)(**Fig. S3F**), this indicates that dasatinib-mediated induction of miR-34a was not transcriptional.

If part of the anti-tumorigenic property of dasatinib is through enhancement of miR-34a activity, then a dasatinib resistant line (MDA-MB-231-Das^R cells; **Fig. 4F**), which has an abrogated response to dasatinib, should harbor lower levels of miR-34a and have weaker miR-34a dasatinib-associated cytotoxicity. Indeed, MDA-MB-231-Das^R cells harbored 3.9-fold lower levels of miR-34a in the presence of 200nM dasatinib(**Fig. 4H**). Additionally, in our clonogenic model, 1 μM dasatinib alone killed ~75% of the MDA-MB-231-Das^R cells(**Fig. 4G**), whereas ~95% kill is observed in parental cells at this dosage. Furthermore, while addition of miR-34a did sensitize the MDA-MB-231-Das^R cells to dasatinib, the effect was milder, with upwards of 15nM miR-34a and 1 μM dasatinib required to evoke a 90% kill (**Fig. 4G**). This value was 98% in parental MDA-MB-231 cells using 10nM miR-34a + 300nM dasatinib. Despite these subtleties, miR-34a significantly sensitized both parental TNBC and Das^R cells to dasatinib. Given that clinical trials utilizing dasatinib in combination with front-line chemotherapeutic agents such as paclitaxel are still ongoing for patients with metastatic breast cancer (NCT00820170 and NCT00924352), we conjecture that addition of a miR-34a agent to these experimental treatment regimens would result in significantly higher response rates.

miR-34a targets the mesenchymal-TNBC specific proto-oncogene c-SRC

Given that dasatinib is a c-SRC inhibitor, the finding that dasatinib promotes miR-34a levels while concomitantly reducing c-SRC levels(**Fig. S3D**), suggests c-SRC in mesenchymal-TNBC cell lines may be part of a feedback loop where c-SRC dampens miR-34a expression and miR-34a directly targets and represses c-SRC(**Fig. S3J**). While there was an inverse correlation between miR-34a and c-SRC levels *in vitro*(**Figs. 1A, S3A, & S3G**), we wanted to determine whether this occurred in tumor samples. We assessed Metabric data, since Illumina mRNA- and Agilent miRNA-microarray data are available on 1,262 patient samples. Spearman rank correlation analysis identified anti-correlation between *SRC* and miR-34a levels ($\rho=-0.064$; $n=1262$; $p<0.008$; **Fig. S3H**). TCGA data was also assessed, however we found no significant anti-correlation ($\rho=-0.01$; $p=0.33$), which may be due to the smaller sample size ($n=632$).

We then looked for miR-34a target sites within the *SRC* 3'UTR using miRNA prediction algorithms and found three putative target sites(**Fig. 5A**). We performed 3'UTR luciferase targeting assays whereby the *SRC* 3'UTR was cloned into pLightSwitch. Co-transfection experiments in HEK-293T cells indicated a dose-dependent reduction in luciferase activity in miR-34a transfected cells(**Fig. 5B**). This effect was not observed on an Empty-3'UTR control or in miR-Scr control transfected cells. Additional mutational analysis of the *SRC* 3'UTR by Muppala *et al.*(33), indicated that miR-34a-induced repression of *SRC* 3'UTR luciferase activity was predominately mediated by the middle miR-34a binding site depicted in **Figure 5A**, which is also the most conserved out of the three target sites according to TargetScan. Importantly, 72 hours post-miR-34a transfection, MDA-MB-231, MDA-MB-436, and BT-549 cells harbored 5.6-, 2.0-, and 4.4-fold reductions in *SRC* transcript levels, respectively(**Fig. 5C**). Reductions in c-SRC protein expression, as well as the *SRC*-regulated gene β -catenin, were also observed in miR-34a transfected TNBC cells but not in luminal-A MCF-7 cells(**Fig. 5D**). Additionally, miR-34a treated MDA-MB-231-derived tumors from our orthotopic experiments harbored ~1.9-fold reduced *SRC* levels ($p\leq 0.049$), as compared to miR-Scr treated tumors(**Fig. 5E**). Taken together, these results indicate miR-34a and c-SRC are part of a regulatory feedback loop in TNBC cells, whereby enhanced activity of c-SRC results in the concomitant

repression of miR-34a, and yet does not appear to involve upstream kinases since the pTyr-416/SRC ratio was not altered by miR-34a re-introduction(**Fig. S3I**).

Loss of c-SRC in mesenchymal-TNBC cells phenocopies gain of miR-34a

Given these results, loss of c-SRC should result in a phenocopy of the gain of miR-34a in TNBC cells. Indeed, MDA-MB-231 cells transfected with 15nM si-SRC promoted a strong anti-growth and pro-senescent phenotype(**Figs. 5F-H**), similar to miR-34a transfected cells. No effects were observed in 15nM si-Neg control treated cells. This ≥ 2.5 -fold anti-growth phenotype induced by 15nM si-SRC was also observed in additional TNBC lines(**Figs. 5H & S4A-B**), and when using a second c-SRC siRNA(**Fig. S4C**). In normal HFF fibroblasts, SRC knockdown resulted in only a 1.3-fold reduction in cell growth as assayed by crystal violet(**Figs. S4D**). si-SRC transfected TNBC cells also had ~ 2 -fold higher miR-34a levels as compared to si-Neg transfected cells(**Figs. 5J & S4F**), confirming the negative regulatory actions of c-SRC on miR-34a, as highlighted by the dasatinib experiments. SRC knockdown efficiency experiments confirmed si-SRC transfected TNBC cells resulted in ~ 5 -fold or greater reductions in SRC mRNA levels(**Fig. S4G**), as well as significant reductions in c-SRC protein levels(**Fig. 5I & S4C**). When senescence assays were performed in si-SRC-transfected MDA-MB-231 cells we observed a 3.6-fold increase in β -gal positive cells(**Fig. 5G**). In an extended panel of si-SRC-transfected TNBC lines the effects were not as robust(**Fig. S4E**), suggesting loss of a single miR-34a target is not sufficient to induce cytostasis, and that miR-34a regulates multiple proto-oncogene targets in TNBC cells to induce pro-senescent phenotypes.

MDA-MB-231 SRC-ORF lines are less responsive to miR-34a re-introduction

Given that c-SRC is an important proto-oncogene in TNBC regulated by miR-34a, we performed gain-of-function rescue experiments to directly assess the contribution of c-SRC in miR-34a-mediated tumor suppression. We generated stable MDA-MB-231-SRC-ORF-GFP overexpressing cell lines through lentiviral transduction. Here, c-SRC is expressed from an RNA transcript without its native 3'UTR, and therefore is not under the regulatory control of miR-34a, as we computationally

determined potential miR-34a binding sites across the entire SRC transcript via RNAhybrid(34), and found none within the coding region. SRC mRNA levels were >40-fold in the SRC-ORF-GFP lines as compared to a control MDA-MB-231-Empty-GFP overexpressing line, or parental MDA-MB-231 cells(**Fig. S5A**). SRC protein expression was elevated only ~3.0-fold in the SRC-ORF-GFP lines as compared to parental MDA-MB-231 cells(**Fig. 6A**). This mild overexpression of c-SRC is expected, given persistently high levels of c-SRC results in severe cytotoxicity(35), and is supported by our observation that GFP^{high} cell populations cannot be maintained in culture. This also indicates the SRC-ORF-GFP line expresses c-SRC at physiologically appropriate levels. This c-SRC is functional, given we observed morphological changes in these cells including greater frequency of cell rounding accompanied by similar rates of cell growth, as has been reported by others(35). We also observed reduced miR-34a levels in the SRC-ORF-GFP line(**Fig. 6E**), expected given our findings that c-SRC negatively regulates miR-34a.

We performed several functional tests in the presence of exogenous miR-34a or miR-Scr control, to determine if SRC-ORF-GFP cells were resistant to miR-34a effects. SRB assays indicated growth of Empty-GFP cells after miR-34a transfection was reduced 3.4-fold, as compared to miR-Scr control treatment(**Fig. 6B**). However, SRC-ORF-GFP cells only harbored an ~1.5-fold reduction in growth post-miR-34a transfection(**Figs. 6B & S5B**). SRC-ORF-GFP lines were also protected from the effects of miR-34a in soft agar assays. SRC-ORF-GFP cells underwent colony formation with greater efficiency than Empty-GFP lines, as determined by the 1.3-fold increase in colony number(**Fig. 6C**), and by the increased colony size. While miR-34a transfection resulted in a 3.5-fold decrease in colony formation in the Empty-GFP line, miR-34a induced only an ~1.3-fold decrease within the SRC-ORF-GFP line. Therefore we conclude overabundance of c-SRC prevents miR-34a-mediated inhibition of anchorage-independent cell growth.

We next tested whether SRC-ORF-GFP lines had a blunted response to the effects of miR-34a on cell invasion(**Fig. 6D**). Similar to parental MDA-MB-231 cells, Empty-GFP lines transfected with miR-34a resulted in a 2.4-fold inhibition of invasion. At baseline, SRC-ORF-GFP cells had ~2.5-fold

greater rates of invasion than Empty-GFP cells, as would be expected given the pro-migratory phenotypes conferred by c-SRC through activation of FAK, RhoA, and PAK signaling(36). However, miR-34a only conferred a 1.2-fold reduction of invasion in the SRC-ORF-GFP cells, indicating gain of c-SRC expression dampens the anti-invasive effects of miR-34a. Overall, these rescue experiments indicate miR-34a regulation of c-SRC partly contributes to the anti-growth effects, but to the majority of the anti-invasive phenotypes mediated by miR-34a re-introduction into TNBC cells.

Identification of a miR-34a gene signature with prognostic value in TNBC

Given the strong anti-tumorigenic effects of miR-34a within TNBC cells *in vitro* and *in vivo*, we asked whether a miR-34a target gene signature could be used as prognostic indicator for TNBC. MDA-MB-231, BT-549, and MDA-MB-436 cells were transfected with either miR-34a or miR-Scr control for 72 hours, and qPCR breast cancer array experiments were performed on RNA isolates(**Fig. 6F**). Since MDA-MB-436 and BT-549 cells were highly correlated with each other(**Fig. S5C**), they were used in the subsequent K-Means clustering analysis(**Fig. S5D**). This analysis identified 4 gene-clusters. Clusters 2 and 3 were most affected by miR-34a re-introduction, since 40–56% of these genes were downregulated ≥ 2 -fold on the qPCR array(**Fig. S5E**). KEGG pathway analysis indicated that 16 out of the 50 genes in Clusters 2 and 3 were involved in “focal adhesion”(**Fig. S5F**), intriguing given mesenchymal-TNBC subtypes harbor a gene expression pattern that includes elevated focal adhesion pathways. Furthermore, in the original hypergeometric analysis, putative miR-34a targets were found to be overrepresented in MSL-and M-TNBC subtypes. This clustering and KEGG analysis indicates that miR-34a re-introduction in these cell lines reduces the expression of focal adhesion genes important in mesenchymal-TNBC biology.

To identify a robust miR-34a gene signature, we asked if the miR-34a downregulated genes identified in Clusters 1-4 were also downregulated in a third cell line, MDA-MB-231, upon miR-34a re-introduction. Using a 2-fold cutoff criterion, seven genes emerged; *BCL2*, *GRB7*, *IGF1R*, *JAG1*, *KRT18*, *NOTCH1*, and *SRC* as being consistently downregulated across 3 separate TNBC lines(**Fig. 6G**). Three of these genes, *BCL2*, *JAG1*, and *NOTCH1*, are known direct targets of miR-34a(37),

while the novel miR-34a target c-SRC discovered in this work was part of this signature as well. Data obtained from Metabric indicated all 7 genes were inversely correlated with miR-34a in TNBC patients (n=203), albeit with some variability in significance(**Fig. S5G**). More important is the finding that this seven-gene signature harbors prognostic value. Using the KM-plotter tool, capable of evaluating survival in 4,142 breast cancer samples(38), we found high expression of these miR-34a targets confers a worse overall survival(**Fig. 6H**). This effect was stronger in TNBC patients (n=245, HR=3.3, p=0.00002) compared to those with Luminal-A tumors (n=611, HR=1.7, p=0.005). The prognostic impact of this gene signature was further validated using a PROGgeneV2 algorithm on TCGA breast cancer data(**Fig. S5H**). Overall, our data supports the idea that re-introduction of miR-34a in mesenchymal-TNBC cell lines promotes anti-tumorigenic phenotypes largely by targeting the proto-oncogene SRC.

Discussion:

In this study, we show miR-34a is dysregulated in TNBC, and when re-introduced can promote tumor-suppressive effects both *in vitro* and *in vivo*. Furthermore, we demonstrated that miR-34a replacement could successfully be performed using tNP technology as a delivery method in mouse xenograft models. MiR-34a imparts these phenotypic effects by targeting *SRC* as well as other *bona-fide* targets such as *BCL2* and *NOTCH1*(39). Moreover, since a double-negative feedback loop exists between c-SRC and miR-34a, TNBC cells can be sensitized to the c-SRC inhibitor dasatinib after miR-34a re-introduction.

miR-34a belongs to the miR-34 family of miRNAs: miR-34a, miR-34b, and miR-34c. *MiR-34a* is located at 1p36 and is encoded in its own transcript, whereas *miR-34b* and *miR-34c* share a primary transcript on 11q23(40). All of these miRNAs share the same seed sequence, and therefore have similar endogenous mRNA targets. The expression of miR-34b and miR-34c is low across all breast cancers, due to allelic deletions and/or the loss of heterozygosity that frequently occurs at 11q23(41,42). Additionally, miR-34a can be epigenetically regulated through promoter

hypermethylation in some breast cancer cell lines and human tumor specimens(43,44). Given the small sample size of these studies, it is still difficult to conclude whether aberrant methylation of miR-34a plays a predominate role in TNBC.

MiR-34a is well established to be under the transcriptional control of the TP53 tumor-suppressive network(45–47). TP53 directly binds the *mir-34a* promoter inducing its expression, while miR-34a indirectly promotes p53 expression by targeting and repressing levels of the deacetylase *SIRT1*, which negatively regulates TP53. Given this positive feed-forward regulatory loop, tumors harboring wild-type TP53 have higher levels of miR-34a than tumors containing a *TP53* mutant allele. Since many TNBC cell lines and tumors harbor *TP53* inactivating mutations, or are *TP53* null, it is not surprising we observed a striking reduction in miR-34a levels within these cell lines and patient samples.

We found both dasatinib and siRNA to c-SRC resulted in enhanced miR-34a levels and activity in TNBC cells. We did not observe similar changes when cells were treated with paclitaxel, and found no evidence for SRC-mediated transcriptional regulation of miR-34a. Furthermore, SRC-ORF overexpressing MDA-MB-231 cells harbored ~2-fold lower miR-34a levels. Together, these data suggest c-SRC, which is highly expressed in TNBC, results in the post-transcriptional dampening of miR-34a levels. Further investigation will be required to decipher the post-transcriptional mechanism by which c-SRC controls miR-34a turnover or decay in TNBC cells. However, since c-SRC can promote PI3K/AKT signaling, miR-34a levels may be controlled by the PI3K/AKT/MDM2 signaling as suggested by Silber *et al.*(48).

We also found miR-34a directly targets c-SRC within its 3'UTR. Re-introduction of miR-34a into TNBC cells significantly reduced *SRC* mRNA levels both *in vitro* and *in vivo*, as well as c-SRC protein levels *in vitro*. These data suggest miR-34a and c-SRC form a double-negative-feedback regulatory loop(**Fig S3J**). Numerous miRNA-mRNA regulatory loops have been identified, and function as an essential regulatory unit that controls the fine-tuning of gene expression important in proper developmental processes(14). In cancer, these feedback loops can become dysregulated,

allowing for a permissive tumorigenic state. In our study, it appears mesenchymal-TNBC cells harboring elevated levels of c-SRC exhibit reduced levels and activity of miR-34a. This may explain why miR-34a re-introduction was able to specifically sensitize mesenchymal-TNBC cells to dasatinib treatment, while it promoted a marginal sensitization to paclitaxel. Furthermore, the impact of miR-34a when re-introduced as a stand-alone agent specifically within the mesenchymal-TNBC subtype was quite striking. Consistent with this effect, hypergeometric analysis indicated MSL- and M-TNBC cells highly express genes that are putative miR-34a targets, more so than other TNBC-subtypes. Overall, these data suggest the pathways aberrantly overexpressed in mesenchymal-TNBC cells important in supporting a pro-tumorigenic state, can also be suppressed by miR-34a, and is why miR-34a levels are found at an extremely low steady-state in these cancers.

Overall, we observed a robust anti-growth, anti-invasion, and pro-cytostatic phenotype occurring in TNBC cells transfected with miR-34a. This complete shutdown of the pro-tumorigenic network indicates numerous genes essential for tumor survival are being downregulated by miR-34a. For instance, we observed downregulation of canonical targets such as *BCL2*, *NOTCH1*, and *IGF1R*(39,49). As highlighted in **Figure 6I**, many of these miR-34a targets were also embedded within the c-SRC signaling pathway, including *SRC* itself, which is activated by integrin and focal adhesion kinase (FAK) signaling. Interestingly, *GRB7*, an adaptor protein important in mediating FAK/SRC signaling was also downregulated by miR-34a in TNBC cells. This effect is predicted to result in a dampening of downstream MAPK and PI3K/AKT signaling pathways important for growth and survival. In support of this, miR-34a treated cells displayed decreases in AKT-regulated genes such as *BCL2* and β -catenin, which are known to be elevated by c-SRC(50). Even the established miR-34a target *NOTCH1* can be controlled by c-SRC during an important processing step involving c-SRC-induced Furin-mediated S1 cleavage of NOTCH1 in the trans-Golgi network(51).

Given the multi-gene targeting occurring in TNBC cells, and from our *in vitro* and *in vivo* data, we conclude that miR-34a could be a promising therapeutic agent for treating TNBC patients. Recently, there has been a major effort to develop small RNAs into therapeutic agents(22,52,53). Our

observations are clinically relevant because an amphoteric liposomal formulation complexed with a synthetic miR-34a mimic (MRX34) is currently being tested in a Phase I clinical trial for patients with hepatocellular carcinoma(54). In pre-clinical models, MRX34 inhibited tumor growth of Hep3B or HuH7 cells orthotopically implanted into the livers of NOD/SCID mice(17). Given miR-34a can target c-SRC and sensitize TNBC cells to dasatinib, our data suggest that the combination of a miR-34a-based therapeutic with dasatinib is worth exploring in future clinical studies of TNBC.

Acknowledgements:

We thank Dr. Leonard Milstone and Jing Zhou for providing the human fibroblast cell line (HFF), Joanna Hu for providing the CRC lines, Lixia Diao for bioinformatic support on the miRNA array analysis, Geoffrey Lyon, Yale Cell Sorter Core Facility, for assistance with FACS sorting and analysis, Amos Brooks, Research Histology & Yale Department of Pathology for the histology and immunohistochemistry, the Firefly Frontiers Grant from Firefly BioWorks for providing funds for miRNA profiling experiments, and Shirin Bahmanyar for providing space and making equipment available for these studies. We also thank Eleni Anastasiadou and Catherine Adams for the critical reading of this manuscript.

References:

1. Liedtke C, Gonzalez-Angulo A, Pusztai L. Definition of triple-negative breast cancer and relationship to basal-like molecular subtype. PPO Updat Princ Pract Oncol. 24(2) ed. New York: Lippincott Williams & Wilkins; 2010;pp. 1–6.
2. Dent R, Trudeau M, Pritchard KI, Hanna WM, Kahn HK, Sawka CA, et al. Triple-negative breast cancer: clinical features and patterns of recurrence. Clin Cancer Res. 2007;13:4429–34.
3. Haffty BG, Yang Q, Reiss M, Kearney T, Higgins SA, Weidhaas J, et al. Locoregional relapse and distant metastasis in conservatively managed triple negative early-stage breast cancer. J Clin Oncol. 2006;24:5652–7.
4. Metzger-Filho O, Sun Z, Viale G, Price KN, Crivellari D, Snyder RD, et al. Patterns of Recurrence and Outcome According to Breast Cancer Subtypes in Lymph Node-Negative Disease: Results From International Breast Cancer Study Group Trials VIII and IX. J Clin Oncol. 2013;JCO.2012.46.1574 – .

5. Perou CM, Sørlie T, Eisen MB, van de Rijn M, Jeffrey SS, Rees CA, et al. Molecular portraits of human breast tumours. *Nature*. 2000;406:747–52.
6. Lehmann BD, Bauer JA, Chen X, Sanders ME, Chakravarthy AB, Shyr Y, et al. Identification of human triple-negative breast cancer subtypes and preclinical models for selection of targeted therapies. *J Clin Invest*. 2011;121:2750–67.
7. Burstein MD, Tsimelzon A, Poage GM, Covington KR, Contreras A, Fuqua S, et al. Comprehensive Genomic Analysis Identifies Novel Subtypes and Targets of Triple-negative Breast Cancer. *Clin Cancer Res*. 2014;21:1688–98.
8. Jiang T, Shi W, Natowicz R, Ononye SN, Wali VB, Kluger Y, et al. Statistical measures of transcriptional diversity capture genomic heterogeneity of cancer. *BMC Genomics*. 2014;15:876.
9. Esquela-Kerscher A, Slack FJ. Oncomirs - microRNAs with a role in cancer. *Nat Rev Cancer*. 2006;6:259–69.
10. Bartel DP. MicroRNAs: genomics, biogenesis, mechanism, and function. *Cell*. 2004;116:281–97.
11. Friedman R, Farh K. Most mammalian mRNAs are conserved targets of microRNAs. *Genome Res*. 2009;19:92–105.
12. Fan M, Krutilina R, Sun J, Sethuraman A, Yang CH, Wu Z-H, et al. Comprehensive Analysis of MicroRNA (miRNA) Targets in Breast Cancer Cells. *J Biol Chem*. 2013;288:27480–93.
13. Davis-Dusenbery BN, Hata A. MicroRNA in Cancer: The Involvement of Aberrant MicroRNA Biogenesis Regulatory Pathways. *Genes Cancer*. 2010;1:1100–14.
14. Adams BD, Kasinski AL, Slack FJ. Aberrant Regulation and Function of MicroRNAs in Cancer. *Curr Biol*. 2014;24:R762–76.
15. Woodrow KA, Cu Y, Booth CJ, Saucier-Sawyer JK, Wood MJ, Saltzman WM. Intravaginal gene silencing using biodegradable polymer nanoparticles densely loaded with small-interfering RNA. *Nat Mater*. 2009;8:526–33.
16. Trang P, Wiggins JF, Daige CL, Cho C, Omotola M, Brown D, et al. Systemic delivery of tumor suppressor microRNA mimics using a neutral lipid emulsion inhibits lung tumors in mice. *Mol Ther J Am Soc Gene Ther*. Nature Publishing Group; 2011;19:1116–22.
17. Daige CL, Wiggins JF, Priddy L, Nelligan-Davis T, Zhao J, Brown D. Systemic delivery of a miR-34a mimic as a potential therapeutic for liver cancer. *Mol Cancer Ther*. 2014;13:2352–60.
18. Zhou J, Patel TR, Fu M, Bertram JP, Saltzman WM. Octa-functional PLGA nanoparticles for targeted and efficient siRNA delivery to tumors. *Biomaterials*. 2012;33:583–91.
19. Zhou J, Liu J, Cheng CJ, Patel TR, Weller CE, Piepmeier JM, et al. Biodegradable poly(amine-co-ester) terpolymers for targeted gene delivery. *Nat. Mater*. Nature Publishing Group; 2011. page 82–90.
20. Palechor-Ceron N, Suprynowicz FA, Upadhyay G, Dakic A, Minas T, Simic V, et al. Radiation induces diffusible feeder cell factor(s) that cooperate with ROCK inhibitor to conditionally reprogram and immortalize epithelial cells. *Am J Pathol*. 2013;183:1862–70.
21. Debnath J, Muthuswamy SK, Brugge JS. Morphogenesis and oncogenesis of MCF-10A mammary epithelial acini grown in three-dimensional basement membrane cultures. *Methods*. 2003. page 256–68.
22. Kasinski AL, Kelnar K, Stahlhut C, Orellana E, Zhao J, Shimer E, et al. A combinatorial microRNA therapeutics approach to suppressing non-small cell lung cancer. *Oncogene*. 2014;

23. Kato M, Paranjape T, Müller RU, Ullrich R, Nallur S, Gillespie E, et al. The mir-34 microRNA is required for the DNA damage response in vivo in *C. elegans* and in vitro in human breast cancer cells. *Oncogene*. 2009;28:2419–24.
24. Humphries B, Wang Z, Oom AL, Fisher T, Tan D, Cui Y, et al. MicroRNA-200b targets protein kinase C α and suppresses triple-negative breast cancer metastasis. *Carcinogenesis*. 2014;00:1–10.
25. Castilla MÁ, Díaz-Martín J, Sarrió D, Romero-Pérez L, López-García MÁ, Vieites B, et al. MicroRNA-200 Family Modulation in Distinct Breast Cancer Phenotypes. *PLoS One*. 2012;7.
26. Lewis BP, Burge CB, Bartel DP. Conserved seed pairing, often flanked by adenosines, indicates that thousands of human genes are microRNA targets. *Cell*. 2005;120:15–20.
27. Ewald JA, Desotelle JA, Wilding G, Jarrard DF. Therapy-induced senescence in cancer. *J. Natl. Cancer Inst.* 2010. page 1536–46.
28. Calvano Filho CMC, Calvano-Mendes DC, Carvalho KC, Maciel GA, Ricci MD, Torres AP, et al. Triple-negative and luminal A breast tumors: differential expression of miR-18a-5p, miR-17-5p, and miR-20a-5p. *Tumor Biol*. 2014;
29. Farazi TA, Horlings HM, Ten Hoeve JJ, Mihailovic A, Halfwerk H, Morozov P, et al. MicroRNA sequence and expression analysis in breast tumors by deep sequencing. *Cancer Res*. 2011;71:4443–53.
30. De Rinaldis E, Gazinska P, Mera A, Modrusan Z, Fedorowicz GM, Burford B, et al. Integrated genomic analysis of triple-negative breast cancers reveals novel microRNAs associated with clinical and molecular phenotypes and sheds light on the pathways they control. *BMC Genomics*. 2013;14:643.
31. Hashimi ST, Fulcher JA, Chang MH, Gov L, Wang S, Lee B. MicroRNA profiling identifies miR-34a and miR-21 and their target genes JAG1 and WNT1 in the coordinate regulation of dendritic cell differentiation. *Blood*. 2009;114:404–14.
32. Navarro F, Gutman D, Meire E, Cáceres M, Rigoutsos I, Bentwich Z, et al. miR-34a contributes to megakaryocytic differentiation of K562 cells independently of p53. *Blood*. 2009;114:2181–92.
33. Muppala S, Mudduluru G, Leupold JH, Buergy D, Sleeman JP, Allgayer H. CD24 Induces Expression of the Oncomir miR-21 via Src, and CD24 and Src Are Both Post-Transcriptionally Downregulated by the Tumor Suppressor miR-34a. *PLoS One*. 2013;8:e59563.
34. Krüger J, Rehmsmeier M. RNAhybrid: MicroRNA target prediction easy, fast and flexible. *Nucleic Acids Res*. 2006;34:451–4.
35. Kato G, Maeda S. High-level expression of human c-Src can cause a spherical morphology without loss of anchorage-dependent growth of NIH 3T3 cells. *FEBS Lett*. 1997;411:317–21.
36. Playford MP, Schaller MD. The interplay between Src and integrins in normal and tumor biology. *Oncogene*. Nature Publishing Group; 2004;23:7928–46.
37. Hsu S Da, Tseng YT, Shrestha S, Lin YL, Khaleel A, Chou CH, et al. MiRTarBase update 2014: An information resource for experimentally validated miRNA-target interactions. *Nucleic Acids Res*. 2014;42.
38. Gyórfy B, Surowiak P, Budczies J, Lánczky A. Online survival analysis software to assess the prognostic value of biomarkers using transcriptomic data in non-small-cell lung cancer. *PLoS One*. 2013;8:e82241.
39. Misso G, Teresa M, Martino D, Rosa G De, Farooqi AA, Lombardi A, et al. Mir-34 : A New Weapon Against Cancer ? *Mol Ther Nucleic Acids*. 2014;3:e194.

40. Hermeking H. The miR-34 family in cancer and apoptosis. *Cell Death Differ.* 2010;17:193–9.
41. Laake K, Launonen V, Niederacher D, Gudlaugsdottir S, Seitz S, Rio P, et al. Loss of heterozygosity at 11q23.1 and survival in breast cancer: results of a large European study. Breast Cancer Somatic Genetics Consortium. *Genes Chromosomes Cancer.* 1999;25:212–21.
42. Newsham IF. The long and short of chromosome 11 in breast cancer. *Am J Pathol.* 1998;153:5–9.
43. Lodygin D, Tarasov V, Epanchintsev A, Berking C, Knyazeva T, Körner H, et al. Inactivation of miR-34a by aberrant CpG methylation in multiple types of cancer. *Cell Cycle.* 2008;7:2591–600.
44. Vogt M, Munding J, Grüner M, Liffers ST, Verdoodt B, Hauk J, et al. Frequent concomitant inactivation of miR-34a and miR-34b/c by CpG methylation in colorectal, pancreatic, mammary, ovarian, urothelial, and renal cell carcinomas and soft tissue sarcomas. *Virchows Arch.* 2011;458:313–22.
45. Tarasov V, Jung P, Verdoodt B, Lodygin D, Epanchintsev A, Menssen A, et al. Differential regulation of microRNAs by p53 revealed by massively parallel sequencing: miR-34a is a p53 target that induces apoptosis and G1-arrest. *Cell Cycle.* 2007;6:1586–93.
46. Bommer GT, Gerin I, Feng Y, Kaczorowski AJ, Kuick R, Love RE, et al. p53-Mediated Activation of miRNA34 Candidate Tumor-Suppressor Genes. *Curr Biol. Elsevier;* 2007;17:1298–307.
47. Raver-Shapira N, Marciano E, Meiri E, Spector Y, Rosenfeld N, Moskovits N, et al. Transcriptional activation of miR-34a contributes to p53-mediated apoptosis. *Mol Cell.* 2007;26:731–43.
48. Silber J, Jacobsen A, Ozawa T, Harinath G, Pedraza A, Sander C, et al. MiR-34a repression in proneural malignant gliomas upregulates expression of its target PDGFRA and promotes tumorigenesis. *PLoS One.* 2012;7.
49. Helwak A, Kudla G, Dudnakova T, Tollervey D. Mapping the Human miRNA Interactome by CLASH Reveals Frequent Noncanonical Binding. *Cell.* 2013;153:654–65.
50. Karni R, Gus Y, Dor Y, Meyuhas O, Levitzki A. Active Src elevates the expression of beta-catenin by enhancement of cap-dependent translation. *Mol Cell Biol.* 2005;25:5031–9.
51. Ma YC, Shi C, Zhang YN, Wang LG, Liu H, Jia HT, et al. The tyrosine kinase c-Src directly mediates growth factor-induced Notch-1 and Furin interaction and Notch-1 activation in pancreatic cancer cells. *PLoS One.* 2012;7.
52. Cheng CJ, Bahal R, Babar IA, Pincus Z, Barrera F, Liu C, et al. MicroRNA silencing for cancer therapy targeted to the tumour microenvironment. *Nature.* 2015;518:107–10.
53. Xue W, Dahlman JE, Tammela T, Khan OF, Sood S, Dave A, et al. Small RNA combination therapy for lung cancer. *Proc Natl Acad Sci U S A.* 2014;111:E3553–61.
54. Bader AG. miR-34 - a microRNA replacement therapy is headed to the clinic. *Front Genet.* 2012;3:120.
55. Halbritter F, Kousa AI, Tomlinson SR. GeneProf data: A resource of curated, integrated and reusable high-throughput genomics experiments. *Nucleic Acids Res.* 2014;42:851–8.

Figure Legends:

Figure 1. miR-34a is aberrantly expressed in mesenchymal-TNBC and is prognostic

A, qPCR analysis of miR-34a levels in normal breast (*gray*), Luminal-A cancer (*blue*), Basal cancer (*red*) cell lines. **B and C**, Kaplan-Meier and Cox-regression analysis of miR-34a levels and overall survival in TNBC (**B**) or all (**C**) breast cancer patients from TCGA datasets. **D**, Hypergeometric analysis(55) of miR-34a targets present within each TNBC-subtype as compared all highly expressed TNBC genes. Specifically, Venn diagrams depict the top 20% most abundant TNBC genes (*yellow*) and TNBC-subtype genes (*green*) from Pietenpol *et al.*(6) as compared to all putative miR-34a targets (*red*). Table depicts the number of miR-34a targets in all TNBC (Number of Successes in Population), and in each TNBC subtype (Number of Successes in Sample), along with the probabilities of success. The probabilities of having X number, or >X number of miR-34a target sites within each TNBC subtype and compared to all TNBC are reported. $P < 0.05$ was considered significant. **E**, SRB growth curves, where various cell lines were transfected with 30nM miR-34a and assayed at indicated times for enumerating cell abundance. SRB assays were performed three independent times with error bars reflecting SEM for each condition or time point analyzed. P-values were calculated by two-way ANOVA.

Figure 2. miR-34a is tumor-suppressive and promotes cytostasis in mesenchymal-TNBC cells

A, BT-549 and MDA-MB-231 cells were transfected with indicated amounts of miR-Scr or miR-34a mimic, serum starved, and plated into Matrigel-coated Boyden chambers with 5% serum as the chemo-attractant. Values reported are the average number of invaded cells counted per field. **B**, BT-549 and MDA-MB-231 transfected cells were seeded into 0.3% soft agar and after 25 days the number of colonies were counted. **C**, MDA-MB-231 transfected cells (30nM miRNA) were treated with either 20 μ M Camptothecin, 0.1% DMSO vehicle, or left untreated, and stained with FITC-VAD-FMK to detect the percentage of apoptotic cells. MiR-34a cells have a heightened percentage of cells undergoing active caspase cleavage only when concomitantly provided Camptothecin, a

quinolone alkaloid known to induce apoptosis. Values under each FACS plot indicate average number or apoptotic events per condition +/- SEM. **D**, MDA-MB-231 transfected cells at indicated times and dose were stained with PI for cell cycle analysis. Numbers in bar graphs represent average percent of cells within each stage of cell cycle, and as a fraction of the total population within each condition. **E**, MDA-MB-231 cells, 6 days post-transfection were stained with SA- β -Gal. Presence of blue perinuclear staining emerged in the miR-34a condition (left panel), which is quantified as an average number of SA- β -Gal positive cells from three independent experiments +/- SEM (right panel). * Indicates $p < 0.01$, as compared to control conditions.

Figure 3. tNP-packaged miR-34a nanoparticles harbor therapeutic efficacy *in vivo*

A, *CrTac:NCr-Foxn1^{nu}* mice containing subcutaneously implanted MDA-MB-231 cells embedded in Matrigel were treated intratumorally with NLE-packaged miR-34a or miR-Scr control particles at a 25 μ g/tumor dose (left panel). Green arrows indicate treatment times. At end of study tumor weights were collected (right panel). All data are depicted as an average tumor size from 8 mice +/- SEM. **B**, *CrTac:NCr-Foxn1^{nu}* mice containing orthotopically implanted MDA-MB-231 cells were treated with tNP-packaged miR-34a or miR-Scr control particles. Green arrows indicate times at which mice were given tail vein injections of miRNA-tNP particles at a 1.35mg/kg dose. Tumor weights are depicted in right panel. All data are depicted as an average tumor size from 8 mice +/- SEM. **C and D**, miRNA (**C**) and target mRNA (**D**) analysis of tumor RNA from each treatment cohort in the miRNA-tNP trial, n=6, ** indicates $p < 0.05$. **E**, Representative H&E (top) and Ki67 (bottom) staining images from treated mice; scale bars, 100 μ m. Ki67 staining is depicted as an average score (n=6). **F and G**, MiRNA toxicity studies. Liver panel analysis on mouse serum from each miRNA-tNP treatment cohort (n=5) (**F**), and representative images of liver tissue stained with H&E (top) and TUNEL (bottom); scale bars, 100 μ m (**G**).

Figure 4. miR-34a sensitizes mesenchymal-TNBC cells to dasatinib

A-C, Clonogenic assays were performed in mesenchymal-TNBC MDA-MB-231 (**A**) and BT-549 cells (**B**), as well as LAR-TNBC MDA-MB-453 cells (**C**). After 10nM miR-34a (red line) or miR-Scr (blue line) transfection, cells were plated at low cell densities in 0-900nM dasatinib (left panels), or 0-4nM paclitaxel (right panels), and resultant colonies were counted 10 days later. Data are presented as the surviving fraction as relative to the 0nM condition for each miRNA treatment condition. (**D**) qPCR assessment of miR-34a levels in dasatinib treated MDA-MB-231 cells for 60 hours. (**E**) miR-34a activity assays using a psiCheck2 3'UTR luciferase reporter in MDA-MB-231 cells. Cells were transfected with sensor constructs (WT=fully complementary miR-34a element (red), or a MUT=mutated miR-34a element (blue)) and treated with the indicated dasatinib doses for 48hrs. (**F**) Dasatinib IC₅₀ curves of MDA-MB-231-Das^R cells (green line), dasatinib sensitive parental MDA-MB-231 cells (red line), and dasatinib insensitive MCF-7 cells (black line). (**G**) Clonogenic assays performed in MDA-MB-231-Das^R cells, with indicated doses of dasatinib. (**H**) qPCR assessment of miR-34a levels in MDA-MB-231-Das^R or parental cells either pulsed or maintained continuously in 100nM dasatinib for 60hrs. P-values of clonogenic assays were calculated by two-way ANOVA. * Indicates p<0.05, as compared to control conditions.

Figure 5. The proto-oncogene c-SRC is a target of miR-34a

A, Schematic depicting the human SRC 3'UTR using the indicated miRNA targeting algorithms, where blue boxes indicated conserved sites, and orange boxes are non-conserved sites. **B**, 3'UTR luciferase assays whereby 293T cells were co-transfected with either an Empty or full length SRC 3'UTR luciferase construct along with miRNA mimics at the doses as indicated. **C-D**, qPCR assessment of SRC mRNA levels (**C**) and western blot analysis of c-SRC expression (**D**) 72 hours post 10nM miR-34a transfection in the indicated cell lines. **E**, c-SRC mRNA levels from orthotopically implanted MDA-MB-231 tumors after miR-34a-tNP treatment. **F**, MDA-MB-231 cells transfected with 15nM si-SRC or si-Neg control, and after 5 days cells were fixed and stained with crystal violet. **G**, Quantification of SA- β -gal activity in MDA-MB-231 cells 6 days post 15nM siRNA

transfection. **H-J**, Characterization of siRNA transfected TNBC cells (15nM) by SRB growth assays (**H**), siRNA knockdown efficiency by western blot analysis (**I**) (Neg=si-Neg, and Si=si-SRC), and by assessment of miRNA levels via qPCR (**J**). In all experiments cells were transfected with 15nM siRNA, and assayed 72 hours post-transfection unless indicated otherwise. Values below each western blot represent the mean densitometric measurement of band intensities relative to the miR-Scr control treatment within each cell line. The numbers highlighted in red indicate SRC/ β -actin ratios for each condition. * Indicates $p < 0.05$, as compared to control conditions. P-values of SRB assays were calculated by two-way ANOVA.

Figure 6. c-SRC overexpression rescues miR-34a-induced phenotypes and is part of miR-34a gene signature

A, Western blot analysis measuring c-SRC, β -catenin, and GAPDH expression in c-SRC-ORF (ORF), GFP-EMPTY (GFP), and parental (Par) MDA-MB-231 cell lines. Values below each blot represent the mean densitometric measurement. **B-D**, Characterization of SRC-ORF-based rescue experiments. For SRB growth assays, c-SRC-ORF (ORF) and GFP-EMPTY (GFP) lines were transfected with 15nM miR-34a or miR-Scr control, and assayed at indicated time points (**B**). miR-34a transfected c-SRC-ORF (ORF) and GFP-EMPTY (GFP) lines at indicated doses were assayed for growth in soft agar (**C**), for invasion potential in Matrigel-Boyden chamber assays (**D**), and for miR-34a levels via qPCR analysis. **E**, Levels of miR-34 and miR-15a in c-SRC-ORF, GFP-EMPTY, and parental MDA-MB-231 cell lines. **F**, Heat map representing log₂ transformed qPCR array data from TNBC cells 72 hours post-transfection with either 10nM miR-Scr or miR-34a. Data was normalized to the geometric mean of B2M and RPLP0 levels, and presented as Euclidean distance with average linkage using CIMminer. **G**, Table depicting a miR-34a gene signature consisting of 7 genes whose expression decreases 2-fold or more when treated with miR-34a, across three different TNBC cell lines. Data originated from qPCR breast cancer array experiments on RNA isolates 72hrs post miR-34a transfection. Values in table represent fold change in gene expression

levels in each cell line relative to the miR-Scr control treatment. TS=TargetScan predicted site, (Score)=context score from TargetScan algorithm. **H**, Kaplan-Meier and Cox-regression analysis of the 7-gene miR-34a gene signature and overall survival in both Luminal-A (*left panel*) and TNBC (*right panel*) breast cancer patients from the KM-plotter Affymetrix array dataset(38). **I**, Diagram depicting the intersection of miR-34a and the c-SRC signaling pathway. Orange boxes indicate receptors, green circles depict intracellular adaptor proteins and kinases, and SRC is highlighted in blue. Experimentally validated miR-34a targets are indicated by italicized green text. For brevity, particular signaling modules are shown as boxes containing keys genes within the pathway. * Indicates $p < 0.05$, as compared to control conditions.

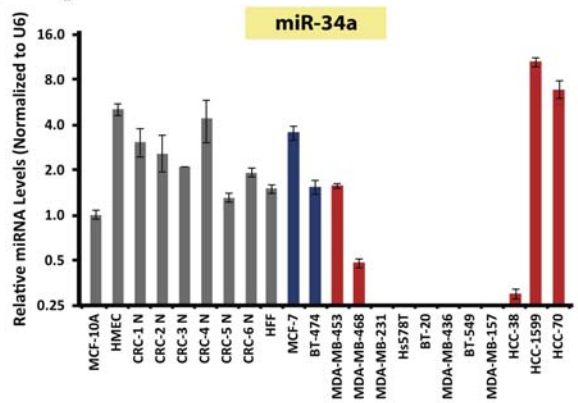
<u>Cell Name</u>	<u>Cell Type</u>	<u>Subtype</u>	<u>miR-34a Level</u>	<u>Relative IC50</u>	<u>Absolute IC50</u>
CRC-Normal	Normal	N/A	++	>20nM	>20nM
MCF-7	Luminal	N/A	++	21.1nM	21.5nM
BT-474	Luminal	N/A	+	28.0nM	32.0nM
MDA-MB-453	Basal	LAR	+	14.5nM	15.0nM
MDA-MB-231	Basal	MSL	--	11.5nM	12.1nM
MDA-MB-157	Basal	MSL	--	7.7nM	8.0nM
MDA-MB-436	Basal	MSL	---	11.0nM	12.1nM
Hs578T	Basal	MSL	--	8.0nM	10.0nM
BT-549	Basal	M	---	6.7nM	7.1nM
BT-20	Basal	Unclassified	-	7.7nM	8.1nM

Table Legends:

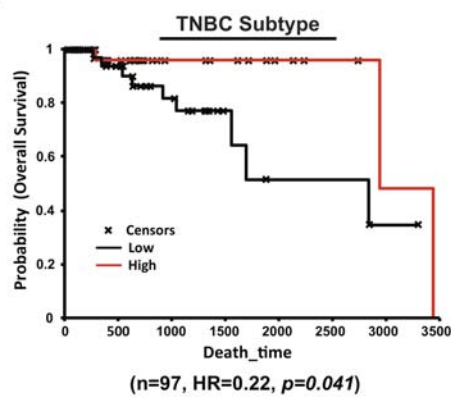
Table 1. IC₅₀ Values for miR-34a re-introduction *in vitro*

++ Indicates high miR-34a expressing lines (\geq 4-fold compared to MCF-10A cells), + indicates moderate miR-34a expression (1-2-fold compared to MCF-10A cells), and -, --, --- indicates low miR-34a expression as determined by 4-, 6-, and 8-fold reductions in levels, as compared to MCF-10A cells.

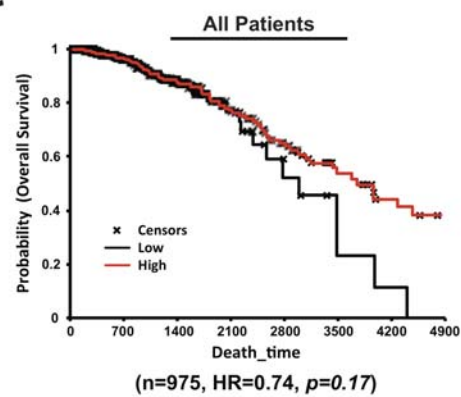
A Figure 1



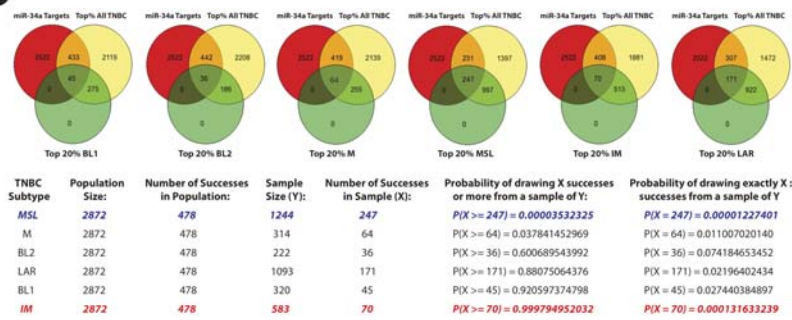
B



C

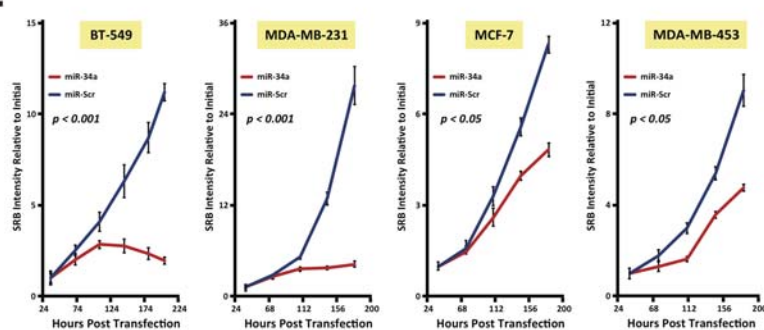


D

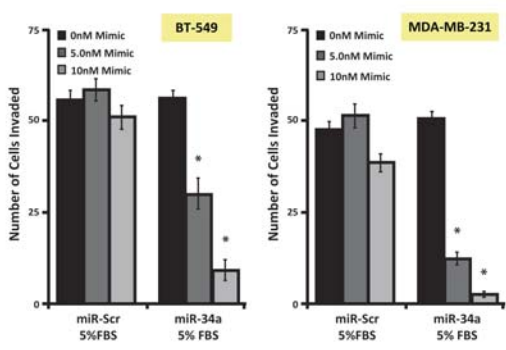


* Top TargetsScan predicted miR-34a targets, irrespective of site conservation, and Context Score cutoff set to -0.05; Number of miR-34a targets = 3000

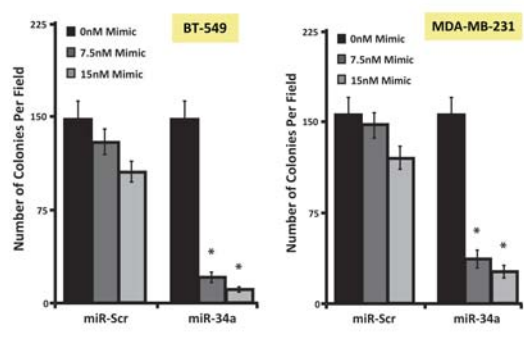
E



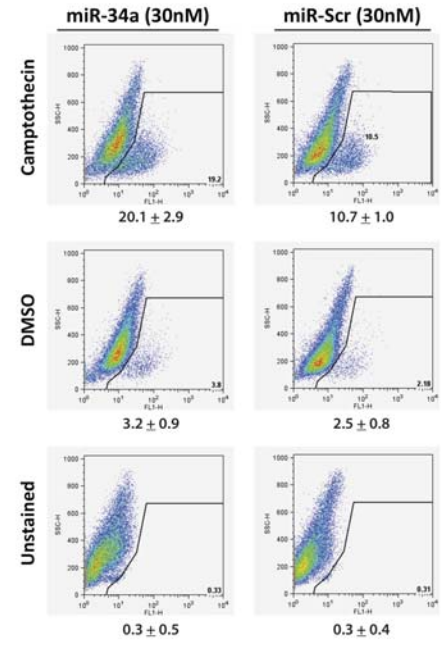
A Figure 2



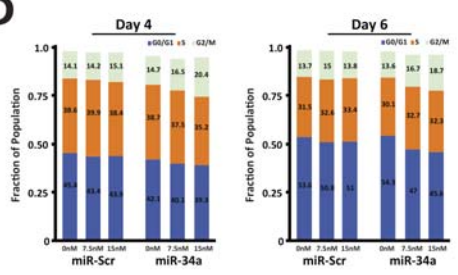
B



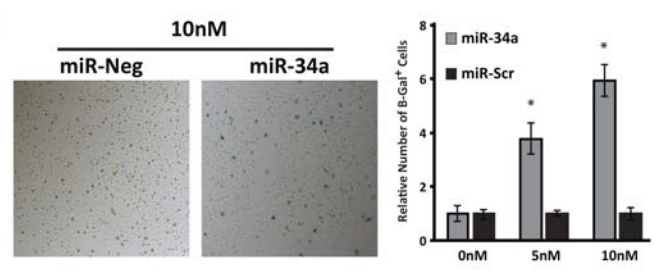
C



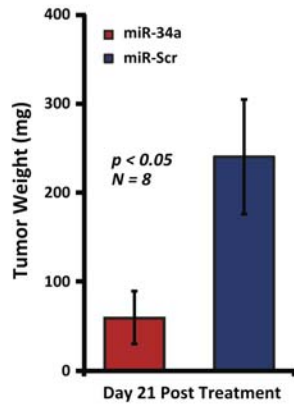
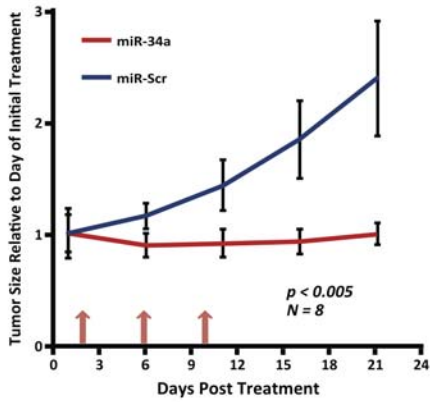
D



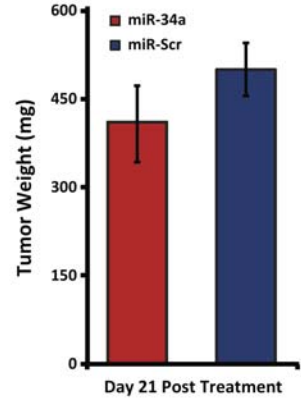
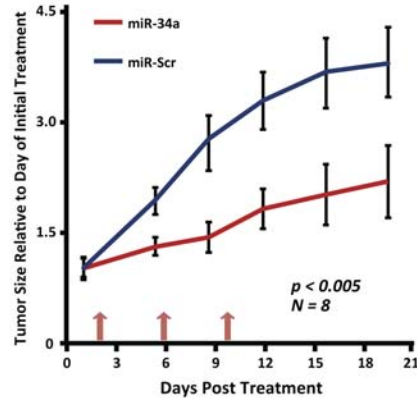
E



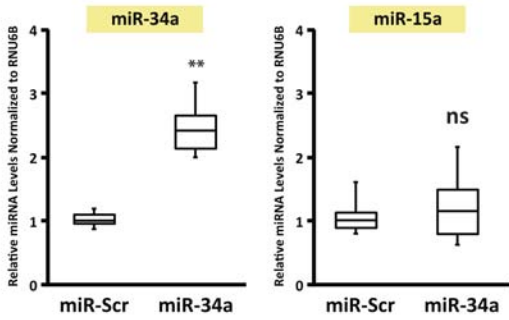
A Figure 3



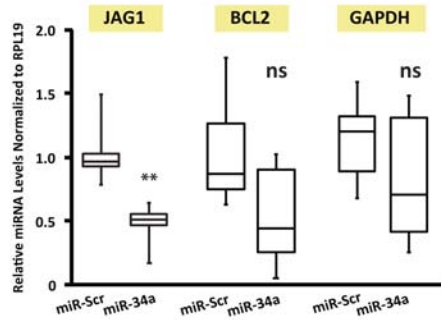
B



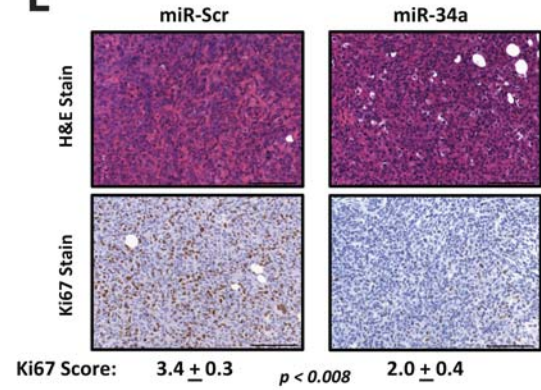
C



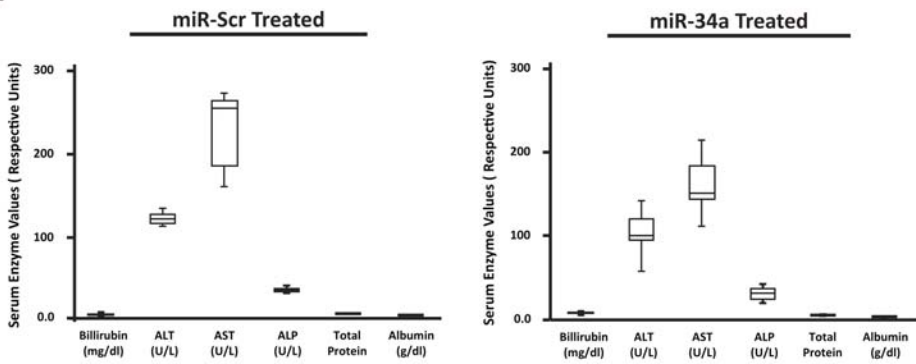
D



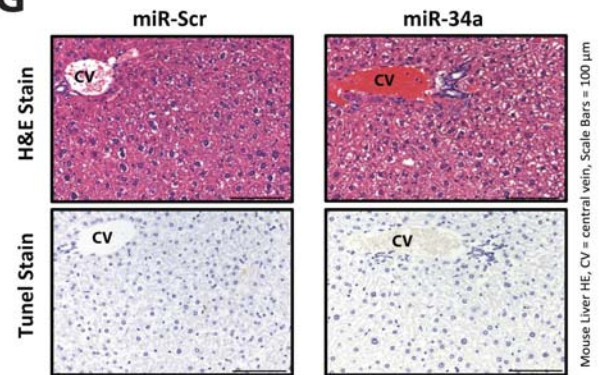
E



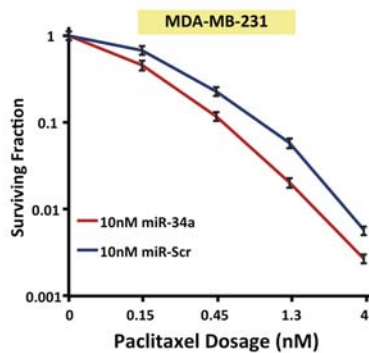
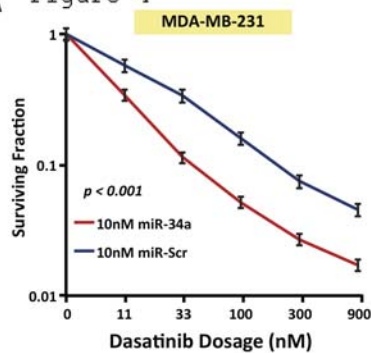
F



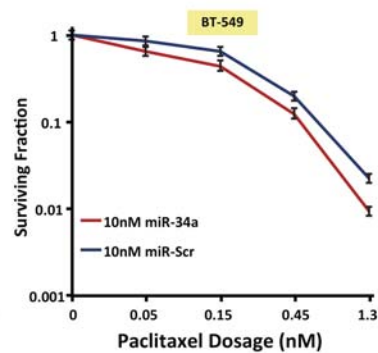
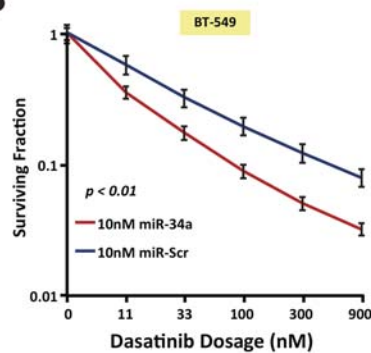
G



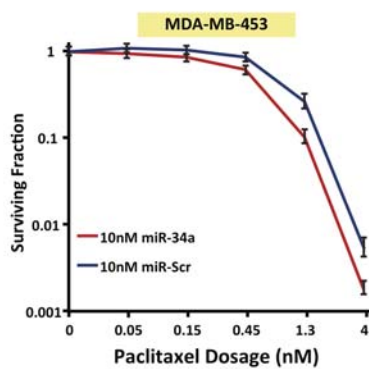
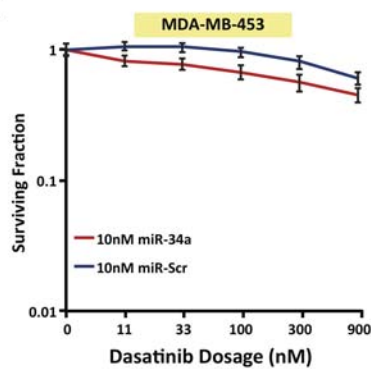
A Figure 4



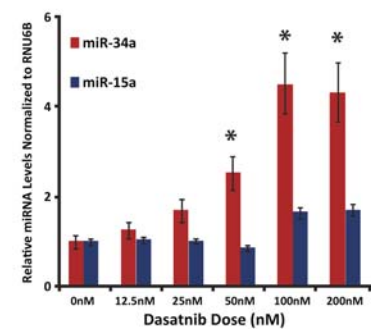
B



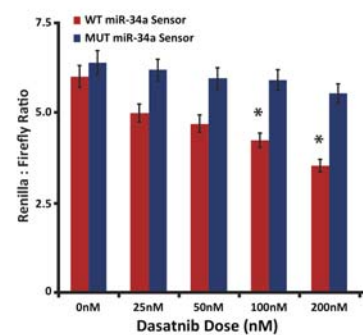
C



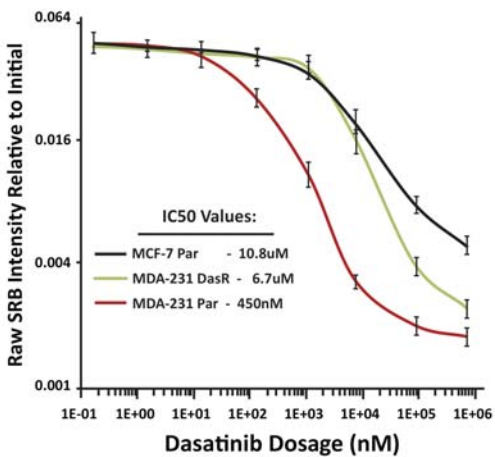
D



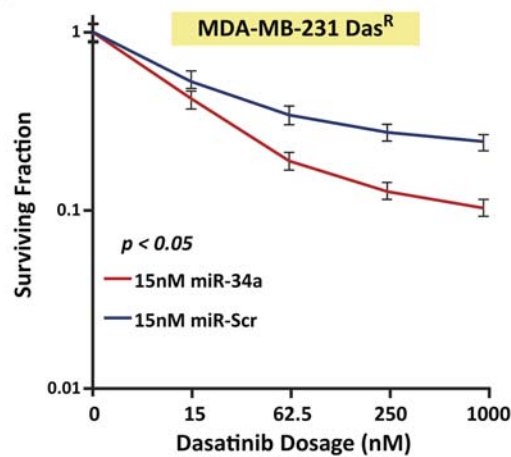
E



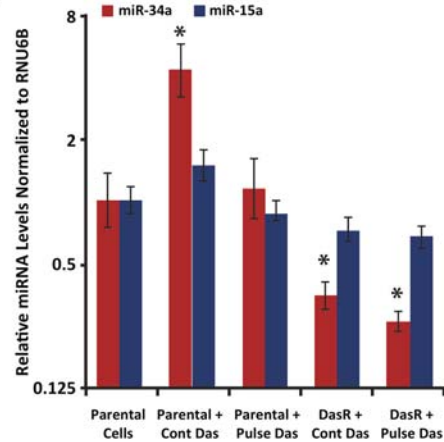
F



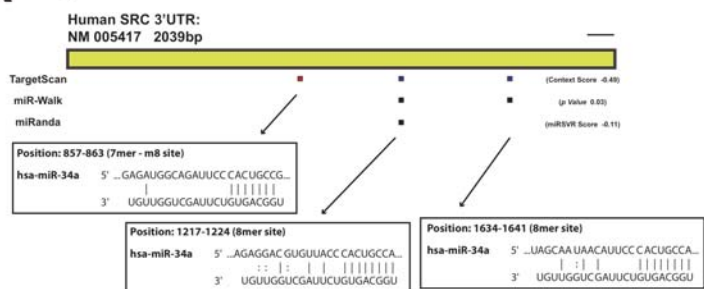
G



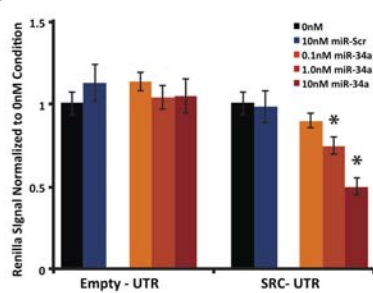
H



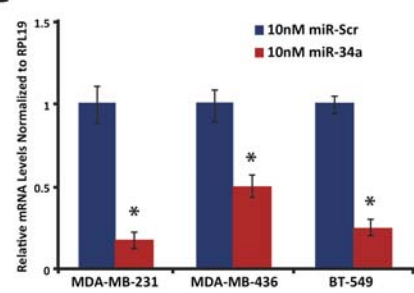
A Figure 5



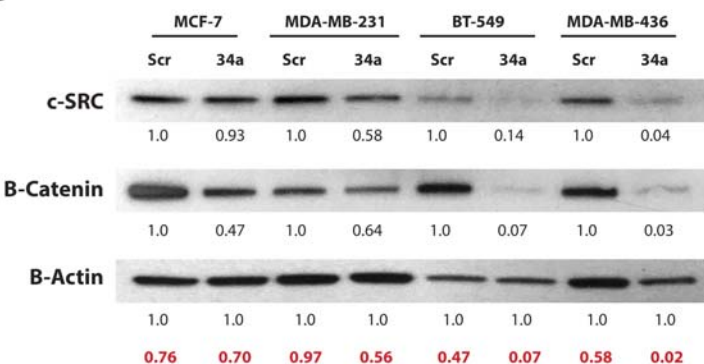
B



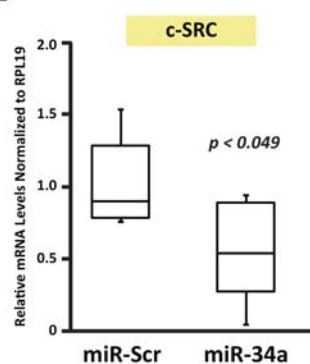
C



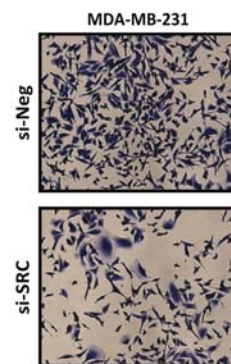
D



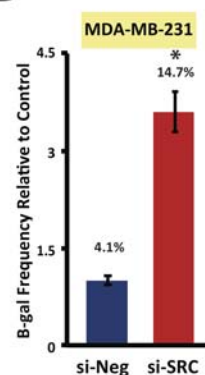
E



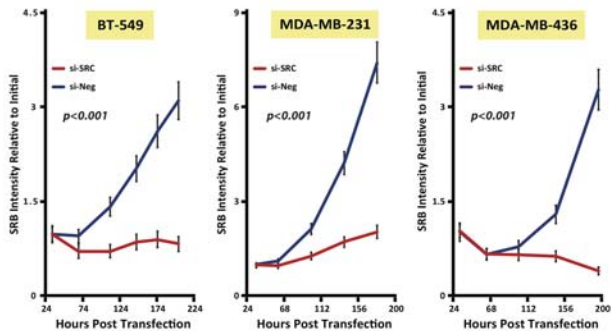
F



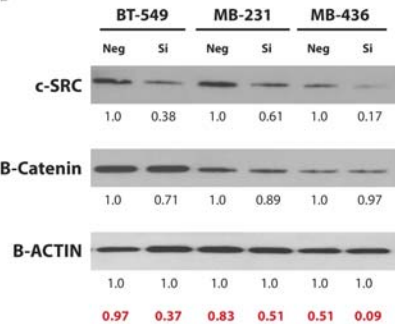
G



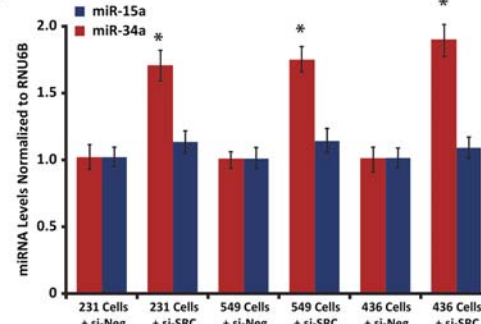
H



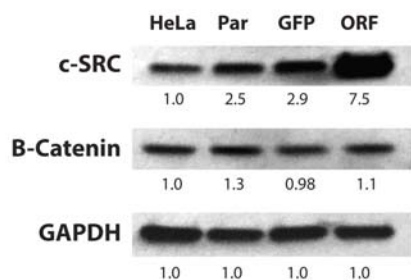
I



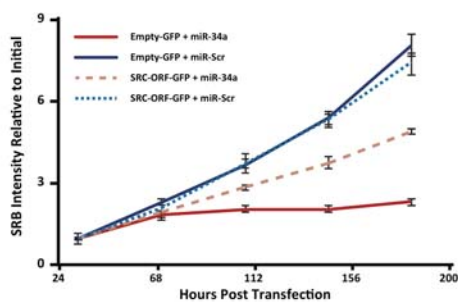
J



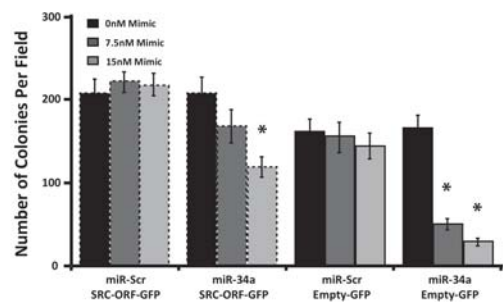
A Figure 6



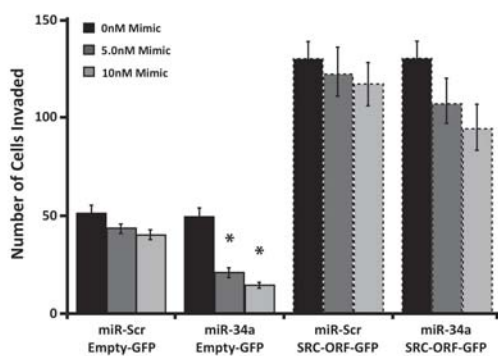
B



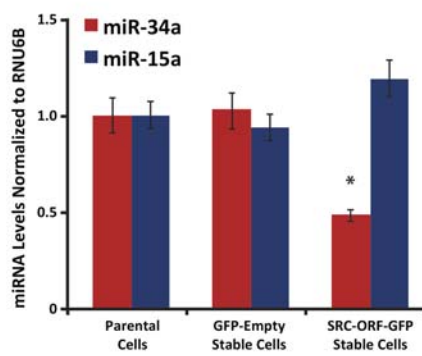
C



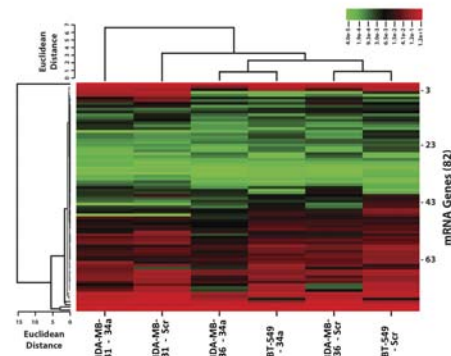
D



E



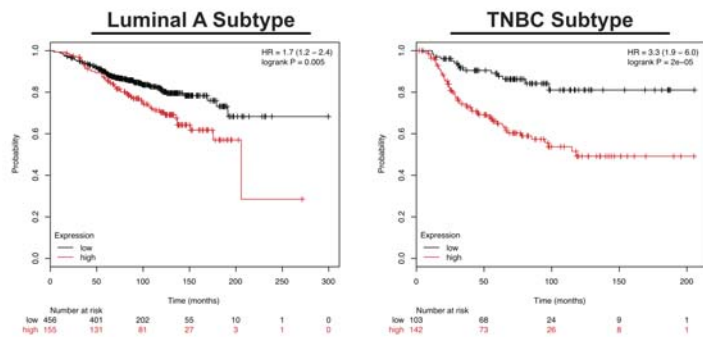
F



G

	KD in 436 & 549	KD in 231	TS Site	(Score)
BCL2	0.33, 0.29	0.43	Y	-0.21
GRB7	0.45, 0.17	0.43	N	
IGF1R	0.31, 0.32	0.44	N	
JAG1	0.17, 0.18	0.42	Y	-0.20
KRT18	0.33, 0.36	0.50	N	
NOTCH1	0.47, 0.25	0.14	Y	-0.44
SRC	0.49, 0.23	0.18	Y	-0.49

H



I

